AIAA JOURNAL
Vol. 31, No. 12, December 1993

Behavior of Laminated Composites Under Monotonically Increasing Random Load

Y. A. Dzenis* and S. P. Joshi†
University of Texas at Arlington, Arlington, Texas 76019
and
A. E. Bogdanovich‡
North Carolina State University, Raleigh, North Carolina 27695

A model using stochastic function theory is proposed to predict the behavior of laminated composites under random loads. Random in-plane loading is defined as a Gaussian process. A numerical procedure for predicting damage evolution and its effect on deformation history of laminated composites is developed. The probabilities of failure of a mesovolume at ply level are used in reducing ply stiffness. The probability of mesovolume failure is calculated based on the theory of excursions of random process beyond the limits. Three modes of failure, i.e., fiber breakage, matrix failure in transverse direction, as well as matrix or interface shear cracking, are taken into account. The results of a numerical study of the effects of loading speed and dispersion on damage evolution and final failure of a Kevlar/epoxy $[0/\pm 30/90]_s$ laminated composite are presented as an illustration. Cases of tension, shear, and complex in-plane loading of the laminate are analyzed for a vast range of loading speeds. The results indicate that the laminate strength and failure strain are higher at higher loading speeds. The analytical results are qualitatively compared with the available experimental observations.

Introduction

DEFORMATION and failure processes in composite structural elements are of a stochastic nature. That fact is due to a number of factors, i.e., inevitable scatters in stiffness and strength properties of components, initial geometric and structural imperfections (particularly, inhomogeneity of arrangement of reinforcing fibers), and stochastic loading. Those factors combined causes scatter in the static and dynamic strength of finite size specimens. On the other hand, for large specimens, where all the possible combinations of random factors are present, they should result in a gradual accumulation of damage and a definite failure strength.

Numerous scientists studied the composite strength problem with the help of statistical modeling (see Refs. 1–3 and references therein). Ovchinskii[1] proposed and worked out the fundamental principles, models, and algorithms for the stochastic simulation of the fracture processes in reinforced composites. However, the simulation procedures with micro-level consideration require extensive computational resources for laminate analysis.

The statistical method for reliability analysis of laminates was developed in Refs. 4–6. In these papers, the theory of random scalar and vector field excursions was applied for computing the probability of excursions of a random stress-strain field beyond the limiting surface. The method was applied in Refs. 7–9 for ply-by-ply stochastic failure analysis and reliability calculation of laminated composite plates and shells. In these papers the whole composite layer was considered as a basic element, and a maximum probability criterion was used for the determination of a damage sequence.

Another approach for a damage accumulation analysis in laminates subjected to deterministic loading was developed by the authors.[10] The model is based on a division of each layer into a statistically large number of mesovolumes. The concentration of broken mesovolumes in plies is calculated as a probability of ply random strains to exceed the limiting failure strains. These concentrations are used in ply stiffness reduction. The model predicts the gradual damage accumulation and deformation history of composite laminates.

In this paper, the combination of approaches in Ref. 10 and Refs. 7–9 is used to describe the behavior of laminated composites under monotonically increasing random loads.

Problem Formulation

Let us consider a symmetric laminate consisting of unidirectionally reinforced laminas with initial random elastic material properties $\tilde{E}_{1_0}^k$, $\tilde{E}_{2_0}^k$, $\tilde{G}_{12_0}^k$, $\tilde{\nu}_{12_0}^k$. The tilde sign denotes the random characteristics, and index k denotes the ply number. We assume the normal distribution of laminas characteristics, therefore we describe them by means of mathematical expectations $\bar{E}_{1_0}^k$, $\bar{E}_{2_0}^k$, $\bar{G}_{12_0}^k$, $\bar{\nu}_{12_0}^k$ and dispersions $D_{E_{1_0}}$, $D_{E_{2_0}}$, $D_{G_{12_0}}$, $D_{\nu_{12_0}}$. Laminate layup is described by ply orientation angle α^k. The load applied to such a system produces a random stress-strain field in the laminas. At some point in loading, a nonzero probability of ply failure emerges, and damages start to accumulate. Accumulation of damages causes the reduction in plies stiffness properties and stress redistribution between plies.

Assume that the applied stresses $\tilde{\sigma}_i(t) = [\tilde{\sigma}_{11}(t), \tilde{\sigma}_{22}(t), \tilde{\tau}_{12}(t)]$ are independent differentiable normal (or Gaussian) processes of time. That assumption means that they can be described by mathematical expectations $\bar{\sigma}_i(t)$ and correlation functions $K_{\sigma_i}(t_1,t_2)$. Assume that the correlation functions depend only on time difference $K_{\sigma_i}(t_1,t_2) = K_{\sigma_i}(t_2 - t_1) = K_{\sigma_i}(\delta)$. The mathematical expectations and correlation functions of derivatives of stresses are related to the same quantities for stresses as follows:

$$\bar{\dot{\sigma}}_i(t) = \dot{\bar{\sigma}}_i(t)$$

$$K_{\dot{\sigma}_i}(\delta) = -\frac{d^2}{d\delta^2} K_{\sigma_i}(\delta) \tag{1}$$

Application of these stresses to a laminate produces a random deformation and stresses in plies $\tilde{\epsilon}_i^k(t)$ and $\tilde{\sigma}_i^k(t)$, respectively. Let us consider the maximum strain failure criterion for ply damage analysis. We have to assess the probability

Received Feb. 12, 1993; revision received April 20, 1993; accepted for publication April 21, 1993.

*Research Associate. Student Member AIAA.
†Associate Professor, Aerospace Engineering Department. Member AIAA.
‡Visiting Scholar, College of Textiles.

of random strains $\epsilon_i^{\sim k}(t)$ in each ply to exceed the limiting strains $\epsilon''^{\sim k}_i$, $\epsilon'^{\sim k}_i$, where the positive $\epsilon'^{\sim k}_i$ (in tension) and negative $\epsilon''^{\sim k}_i$ (in compression) limits are also random in general. This probability can be calculated as

$$r_i^k(t) = 1 - \exp\left[-\int_0^t \nu_i^k(\tau)\, d\tau\right] \tag{2}$$

where $\nu_i^k(t)$ is a mathematical expectation of the number of excursions of $\epsilon_i^{\sim k}(t)$ beyond the interval $[\epsilon''^{\sim k}_i, \epsilon'^{\sim k}_i]$ per unit time. Assuming statistical independence of crossing the negative and positive limits, $\nu_i^k(t)$ can be calculated as a sum of mathematical expectations of these events

$$\nu_i^k(t) = \nu_{i-}^k(t) + \nu_{i+}^k(t) \tag{3}$$

The mathematical expectation of the number of excursions beyond the negative and positive limits can be calculated as[7-9]

$$\begin{aligned}
\nu_{i-}(t) &= \frac{1}{2\pi}\sqrt{\frac{D_{\dot\epsilon_i}}{D_{\epsilon_i}+D_{\epsilon''_i}}}\exp\left\{-\frac{[\bar\epsilon_i(t)-\bar\epsilon''_i]^2}{2(D_{\epsilon_i}+D_{\epsilon''_i})}\right\}\\
&\times\left\{\exp\left[-\frac{\bar{\dot\epsilon}_i(t)^2}{2D_{\dot\epsilon_i}}\right]-\sqrt{\frac{2\pi}{D_{\dot\epsilon_i}}}\bar{\dot\epsilon}_i(t)\Phi\left[-\frac{\bar{\dot\epsilon}_i(t)}{\sqrt{D_{\dot\epsilon_i}}}\right]\right\}\\
\nu_{i+}(t) &= \frac{1}{2\pi}\sqrt{\frac{D_{\dot\epsilon_i}}{D_{\epsilon_i}+D_{\epsilon'_i}}}\exp\left\{-\frac{[\bar\epsilon_i(t)-\bar\epsilon'_i]^2}{2(D_{\epsilon_i}+D_{\epsilon'_i})}\right\}\\
&\times\left(\exp\left[-\frac{\bar{\dot\epsilon}_i(t)^2}{2D_{\dot\epsilon_i}}\right]+\sqrt{\frac{2\pi}{D_{\dot\epsilon_i}}}\bar{\dot\epsilon}_i(t)\left\{1-\Phi\left[-\frac{\bar{\dot\epsilon}_i(t)}{\sqrt{D_{\dot\epsilon_i}}}\right]\right\}\right)
\end{aligned} \tag{4}$$

where

$$\Phi(U) = \frac{1}{\sqrt{2\pi}}\int_{-\infty}^{U} e^{-(u^2/2)}\, du = \frac{1}{2}\left[1+\operatorname{erf}\left(\frac{U}{\sqrt{2}}\right)\right]$$

is the Laplace function; the ply index k is avoided for simplicity. To use formulas (4) we need to have the following information about the ply strains: $\bar\epsilon_i^k(t)$, $\bar{\dot\epsilon}_i^k(t)$, $D_{\epsilon_i}^k$, $D_{\dot\epsilon_i}^k$. Note that the simple relation [Eq. (2)] between the probability of an event and mathematical expectation of the number of events assumes the Poisson-type process of events formation with time. This assumption can be valid for rare independent events. In our case, the use of the formula is justified if the average time spacing between the occurrence of events is larger than the autocorrelation time for the loading process (see Ref. 11).

Assuming that the processes of changing the composite compliances are slow and their derivatives may be neglected, the mathematical expectations and dispersions of laminate deformations and deformation derivatives can be calculated using the properties of random function operators

$$\begin{aligned}
\bar\epsilon_i(t) &= \int_0^t \bar S_{ij}(\tau)\,\bar\sigma_j(\tau)\, d\tau\\
\bar{\dot\epsilon}_i(t) &= \bar S_{ij}(t)\,\bar{\dot\sigma}_j(t)\\
D_{\epsilon_i} &= \bar S_{ij}^2(t)\,K_{\sigma_j}(0) + \bar\sigma^2{}_j(t)\,D_{S_{ij}}\\
D_{\dot\epsilon_i} &= \bar S_{ij}^2(t)\,K_{\dot\sigma_j}(0) + D_{S_{ij}}[\bar{\dot\sigma}_j(t)]^2
\end{aligned} \tag{5}$$

Current laminate compliances may be calculated using the information about the current laminas properties and lamination theory. The full set of formulas derived for an orthotropic laminate and stiffness reduction algorithm is given in Ref. 10. Shear-extension coupling coefficients are obtained by using the calculation procedure outlined for the other coefficients in Ref. 10.

Algorithmic Development

A computer code is developed for calculating laminate response using the previously described approach. Incremental loading is set in the program according to the given stress derivatives $\bar{\dot\sigma}_i(t)$, and the deformation integral (5) is evaluated numerically. On each time step the damage functions $r_i^k(t)$ accumulated up to the previous step are used to calculate the current elastic properties of the material and laminate deformations. The complete failure of the laminate is assumed to occur when any of the current effective elastic moduli $\bar E_1(t)$, $\bar E_2(t)$, or $\bar G_{12}(t)$ becomes equal to zero. The calculated information for each time step is appended to the data file, including the information on laminate stresses, strains, and laminas strains; the damage content $r_i^k(t)$ in plies; the average content of damages of a different type in the laminate $r_i(t) = [\Sigma_{k=1}^n r_i^k(t)]/n$; the cumulative damage content $r_c(t) = [\Sigma_{i=1}^3 r_i(t)]/3$; and the current laminate elastic moduli $\bar E_1(t)$, $\bar E_2(t)$, $\bar G_{12}(t)$. The program is written in "Mathematica" language.

Results and Analysis

The developed computer code is used for the numerical study of the effects of loading speed and dispersion on damage evolution in Kevlar/epoxy $[0/\pm 30/90]_s$ laminate. Experimental statistical data for Kevlar/epoxy unidirectional composite presented in Ref. 12 are used for the mesovolume material properties definition (see discussion on mesovolume properties in Ref. 10).

Effect of Loading Rate

The following cases of stochastic loading of $[0/\pm 30/90]_s$ laminate are analyzed: tension $\tilde\sigma_i(t) = [\tilde\sigma(t), 0, 0]$, compression $\tilde\sigma_i(t) = [-\tilde\sigma(t), 0, 0]$, shear $\tilde\sigma_i(t) = [0, 0, \tilde\sigma(t)]$, biaxial tension $\tilde\sigma_i(t) = [\tilde\sigma(t), \tilde\sigma(t), 0]$, and complex in-plane loading $\tilde\sigma_i(t) = [\tilde\sigma(t), \tilde\sigma(t), \tilde\sigma(t)]$. In all cases the mathematical expectation of loading function $\tilde\sigma(t)$ is the linear function of time, and the correlation function of the process is

$$K_\sigma(\delta) = \sigma_q^2 e^{-\delta^2/\tau_0^2} \tag{6}$$

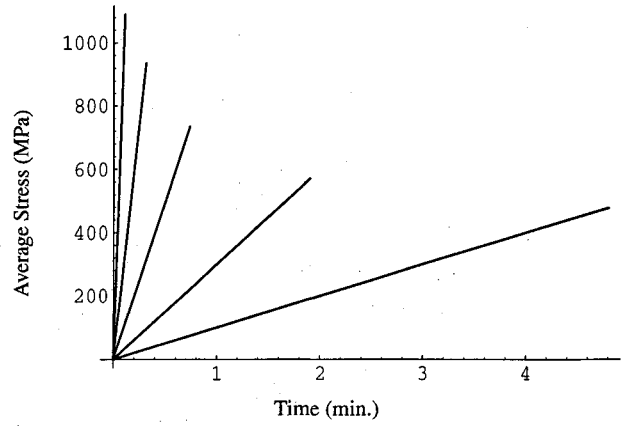

Fig. 1a Applied stress. Arrow points toward curves with higher loading rates.

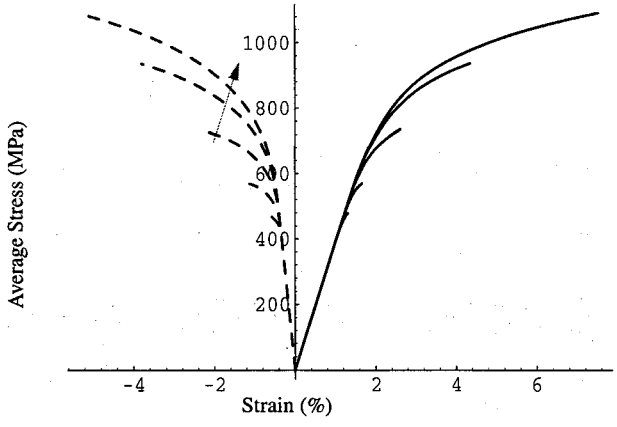

Fig. 1b Stress-strain behavior of the laminate under tension. Arrow points toward curves with higher loading rates.

where $\sigma_q^2 = D_\sigma = K_\sigma(0)$ is the dispersion of the process and τ_0 is the autocorrelation time of random fluctuations of loading. The derivative $\dot{\sigma}(t)$ consequently has a constant mathematical expectation and dispersion $D_{\dot{\sigma}} = K_{\dot{\sigma}}(0) = 2\sigma_q^2/\tau_0^2$. The standard deviation of loading process σ_q is chosen equal to 0.01 GPa. Correlation time is 0.01 min. Several orders of loading rate are covered in the numerical study.

Figure 1 shows stress-strain behavior of a $[0/\pm 30/90]_s$ laminate under the uniaxial tension for five different loading rates ($\dot{\sigma} = 0.1$, 0.3, 1, 3, and 10 GPa/min). Variation of the average damage functions r_i and cumulative damage function r_c with loading for these cases is shown in Fig. 2. In these and several of the following figures, continuous lines, dashed lines, and dash-dot lines correspond to subscripts 11, 22, and 12 of the plotted variables, respectively. The analysis shows that laminate failure strength in tension increases considerably with the increase of loading rate from 0.1 to 10 GPa/min (Fig. 1). Failure strain also increases and deformation behavior becomes more nonlinear with the increase of the loading rate.

The analysis of ply-by-ply damage parameters shows that a small amount of shear cracks appears in ± 30 deg plies first for all loading rates. Shear cracks continue to accumulate slowly in these plies up to the final failure. At the load level of about 100 MPa, rapid transverse cracking of the matrix appears in the 90 deg ply. Then, before the final failure, fiber breakage in the 0 deg ply due to tension and in the 90 deg due to compression, as well as matrix cracking in ± 30 deg plies appear almost simultaneously. With the increase of the loading rate, the onset of damage accumulation is shifted to the higher loading and damage develops over a relatively longer stress range as seen in Fig. 2. It is interesting that at low speeds, there is almost no fiber failure in ± 30 deg plies up to the final failure. But with increasing speed, the fiber failure starts to develop and for $\dot{\sigma} = 10$ GPa/min there are about 87% of mesoelements broken in the fiber mode in these plies at failure. At the same time, the percentage of transverse matrix damage at failure in ± 30 deg plies lowers from almost 100% at 0.1 GPa/min to about 65% at 10 GPa/min. Thus, increasing loading speed may result not only in a shift and stretching of the loading interval of the damage accumulation, but can also cause qualitative changes in the damage sequence.

Figures 3 and 4 show calculated stress-strain diagrams and cumulative damage functions for shear and complex in-plane loading, respectively. The general trend of the increase of failure stress with increasing loading speed is revealed. However, unlike uniaxial tension, for the loading cases shown the failure stresses for loading speeds 3 and 10 GPa/min almost coincide. The shift in damage accumulation onset and the stretching of stress interval of damage accumulation with increase in loading rates are also deduced from all of the information available about damage evolution. The cumulative damage content at failure varies slightly with loading speed and is a little higher for complex multiaxial loading.

The variation of failure stress with loading rate for all of the loading cases is plotted in Fig. 5. Gradual increase of failure stress with increase of loading speed is observed up to the speed about 3–10 GPa/min. For higher speeds the failure stress practically does not depend on loading speed. For these speeds, the mathematical expectation of the number of excursions [Eq. (4)] becomes directly proportional to the mean process speed, and it compensates the shortage of time. Note that at higher speeds the condition of the noncorrelated process and its derivative used in the derivation of [Eq. (4)] may be violated and the present analysis may not be valid.

Effect of Stochastic Deviation in Loading

The effect of randomness in loading on the laminate behavior was investigated on $[0/\pm 30/90]_s$ laminate under tension. The loading rate dependence of failure stress and strain for the laminate under tension with a different stochastic deviation is shown in Fig. 6. Analysis shows that the behavior of failure parameters with respect to the loading rate is strongly affected by the loading deviation. For small loading deviations, the rate dependency of failure stress is observed only for low loading rates. Failure parameters show a stronger dependence on the loading rate for loading with high derivation.

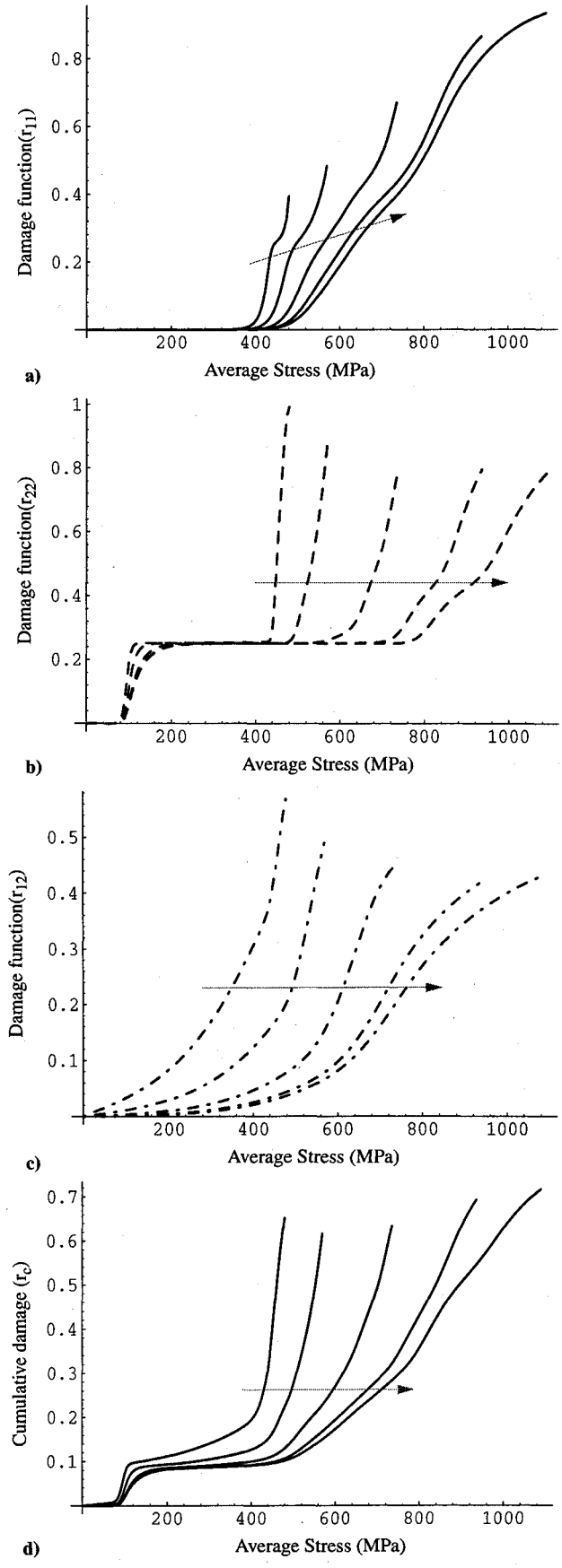

Fig. 2 Damage accumulation in the laminate under tension: a) average fiber, b) average transverse matrix, c) average shear, and d) cumulative damage.

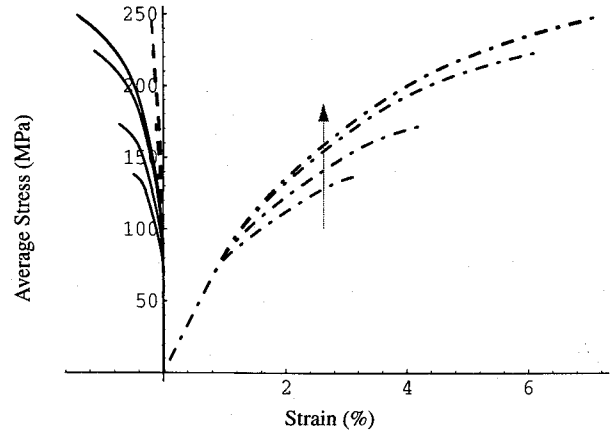

Fig. 3a Stress-strain curves.

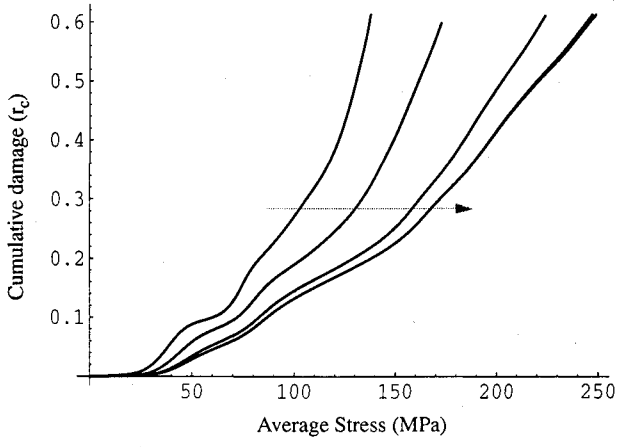

Fig. 3b Cumulative damage accumulation under shear.

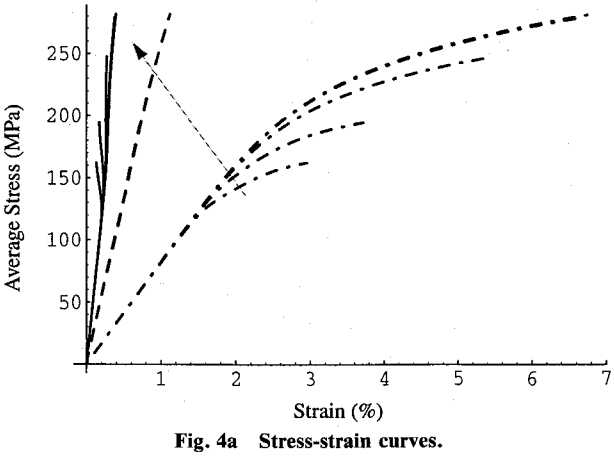

Fig. 4a Stress-strain curves.

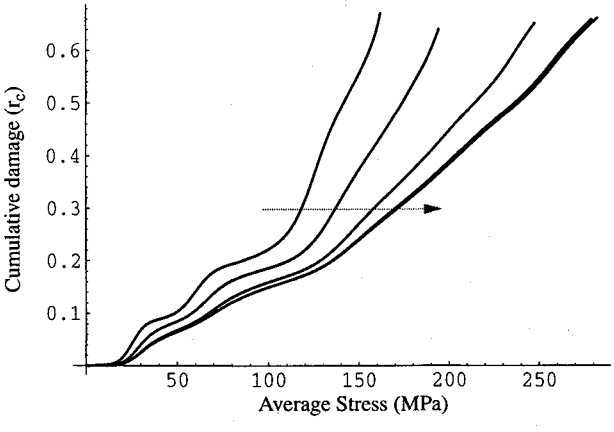

Fig. 4b Cumulative damage accumulation under complex in-plane loading.

For low loading speeds, the increase in stochastic deviation of loading results in lowering failure stress. With the increase of the loading rate, however, the failure stresses for various loading deviations become closer. At higher speeds, the loading with higher deviation causes higher failure stress. The physical interpretation of this observed effect can be the following. At low speeds, increase of stress deviation widens the resulting bands of deformation processes in plies, and that causes the increase of a possibility of process excursion and damage formation, consequently lowering the failure stress. At high speeds, however, when the loading time is comparable to the correlation time of random fluctuations of stress, there is a nonzero probability that the process will be below its mathematical expectation during the whole loading time. And so to reach the unity probability of excursion, the whole process band should exceed the limit. Larger dispersion results in higher mean value of the process at this point. Note that the curves in Fig. 6 show failure parameters for loading processes having the same deviations at different speeds. In reality, it seems natural for a higher-speed process to have a higher deviation.

Damage Induced Anisotropy

The damage processes in $\pm\alpha$ plies of the initially balanced laminate may lead to this laminate becoming unbalanced. For an unbalanced laminate, the $\bar{A}_{16}$, $\bar{A}_{26}$ components of the stiffness matrix are not zero. Therefore it should be taken into account when calculating the compliances, moduli, and laminate deformations. Different damages appear in $\pm\alpha$ plies if the laminate is loaded with shear loading. The effect of shear coupling on the laminate deformation is seen in Figs. 2 and 3. To assess the magnitude of the effect, the variation in $\bar{A}_{16}$, $\bar{A}_{26}$

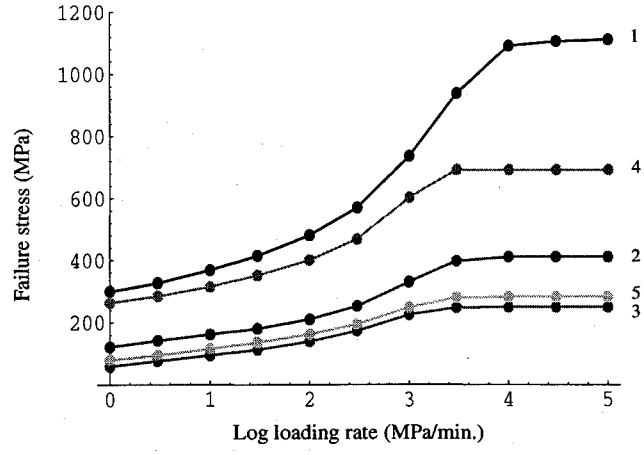

Fig. 5 Variation of failure stress with loading rate: 1—tension, 2—compression, 3—shear, 4—biaxial loading, and 5—complex in-plane loading.

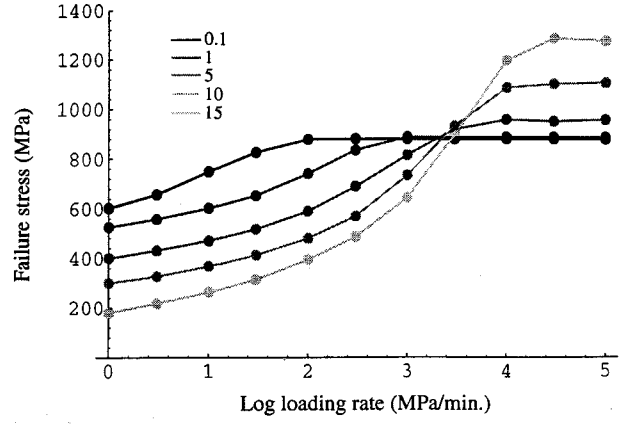

Fig. 6 Variation of failure stress of the laminate under tension with loading rate. Numbers indicate deviation of loading in MPa.

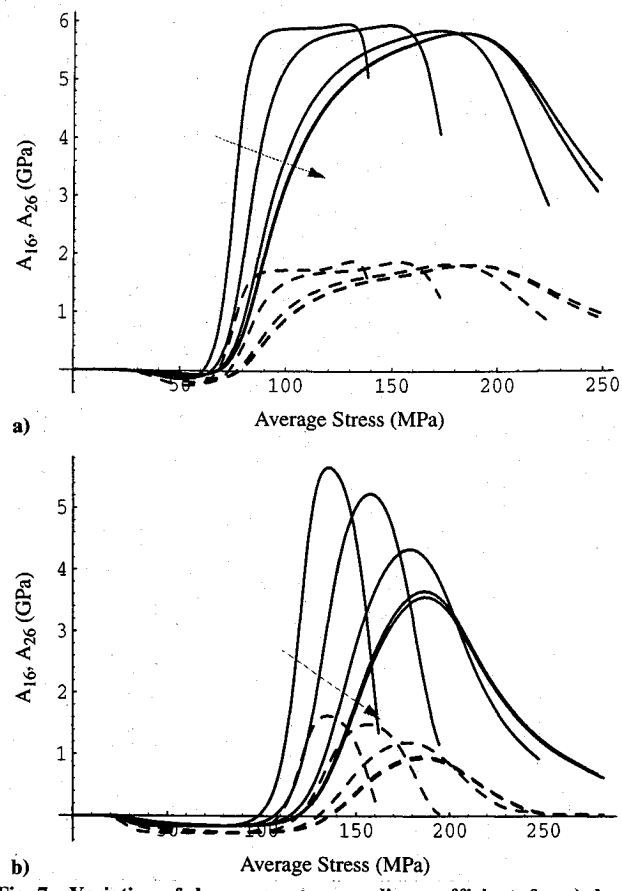

Fig. 7 Variation of shear-extension coupling coefficients for a) shear loading and b) complex in-plane loading. Solid and dashed lines represent A_{16} and A_{26}, respectively.

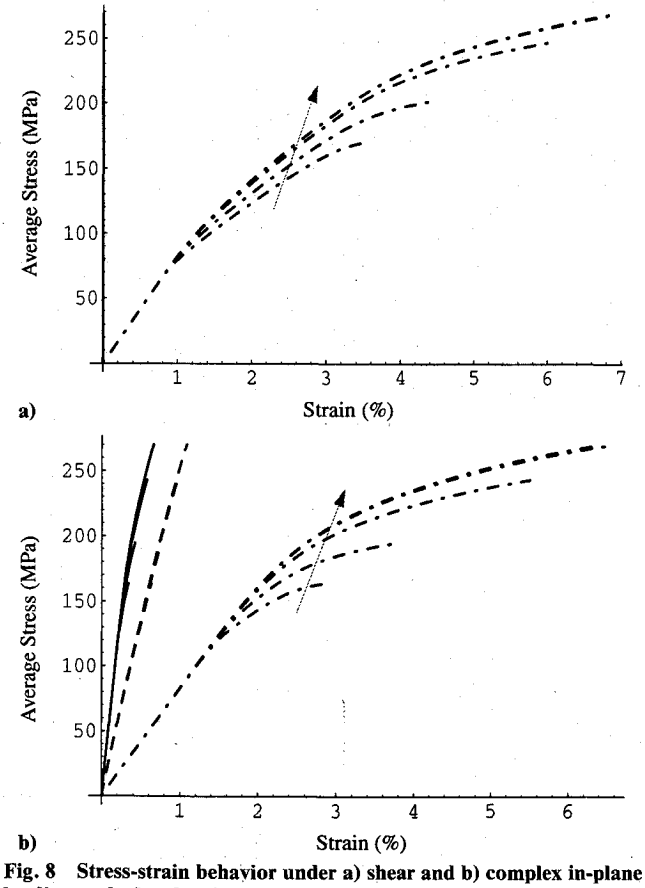

Fig. 8 Stress-strain behavior under a) shear and b) complex in-plane loading calculated without accounting for damage-induced anisotropy.

Table 1 Material properties for the Kevlar/epoxy lamina[12]

Characteristic	Average value	Standard deviation	Relative standard deviation, %
E_1 (GPa)	74.9	2.22	2.97
E_2 (GPa)	4.65	0.16	3.44
G_{12} (GPa)	1.877	0.033	1.76
ν_{12}	0.35	0.031	8.86
ϵ'_{11}	0.0171	0.002	11.7
ϵ''_{11}	−0.00478	0.00024	5.2
ϵ'_{22}	0.00283	0.00016	5.6
ϵ''_{22}	−0.0141	0.0011	7.8
$\gamma'_{12}, \gamma''_{12}$	±0.0256	0.0079	30.8

Table 2 Material properties for SP 250/S-2 glass/epoxy and available properties for Scotchply Type 1002 glass/epoxy shown in parentheses

Characteristic	Average value	Standard deviation	Relative standard deviation, %
E_1 (GPa)	49.4 (39.3)	0.48	0.98
E_2 (GPa)	16.3 (9.7)	0.34	2.11
G_{12} (GPa)	6.35	0.33	5.21
ν_{12}	0.28	0.01	3.57
ϵ'_{11}	0.0318 (0.0246)	0.0018	5.66
ϵ''_{11}	−0.0222 (−0.0224)	0.0006	2.7
ϵ'_{22}	0.003 (0.0021)	0.0009	30.0
ϵ''_{22}	−0.0286 (−0.02)	0.0068	23.8
$\gamma'_{12}, \gamma''_{12}$	±0.0219	0.00149	6.8

is plotted as a function of loading in Fig. 7 for all of the loading rates.

Coefficients $\bar{A}_{16}$, $\bar{A}_{26}$ may become fairly big due to damage accumulation. Thus, the maximal value of $\bar{A}_{16}$ is about 6 GPa, which is comparable to the laminate initial elastic moduli $E_1 = 39.7$ GPa, $E_2 = 23.2$ GPa, and $G_{12} = 8.4$ GPa. In both loading cases, small negative values of these coefficients at a low loading level are due to the matrix transverse damage in the −30 deg ply. The following sharp increase $\bar{A}_{16}$, $\bar{A}_{26}$ is due to fiber breakage in the same ply. The final reduction of coefficients is caused by fiber breakage in the +30 deg ply. The stress-strain diagrams for these loading cases, calculated without taking into account shear coupling, are shown in Fig. 8. The comparison of this figure with Figs. 2 and 3 shows that a calculation without accounting for the shear coupling may lead to overestimation of laminate failure stress up to 20%. The qualitative changes in stress-strain diagrams and in damage accumulation functions are also observed.

Experimental Observations

Staab and Gilat[13] recently investigated the effect of the strain rate on the behavior of Scotchply Type 1002 glass/epoxy in an angle-ply configuration. Tests have been conducted at strain rates of approximately 10^{-5} 1/s and 10^{3} 1/s. The stochastic material property data are not available for the material used in the experimental investigation. Some of the material properties of SP250/S-2 are close to a Scotchply Type 1002 glass/epoxy composite. Use of these material properties in the analysis allows a qualitative comparison of predictions with experimental observations. The material property information for SP250/S-2 glass/epoxy composite necessary for the analysis is given in Table 2. The analysis is performed by assuming the following values for the loading parameters: $\tau = 1$ s, $D_\sigma = 0.5$ MPa, $\dot{\sigma} = 10^4$ GPa/s (fast loading) and $\dot{\sigma} = 10^{-4}$ GPa/s (slow loading). Figures 9–11 compare the experimentally observed stress-strain behavior with the analytically predicted behavior for ±30, ±45, and ±60 angle-ply laminates, respectively. Analytical predictions show the same trend as the experimental observations. The quantitative difference may be due to the difference in stiffness and strength

properties of Scotchply Type 1002 and SP250/S-2 glass/epoxy materials. Table 2 shows the available material properties of Scotchply Type 1002 glass/epoxy in brackets for comparison. The average failure strains for Scotchply Type 1002 glass/epoxy in Table 2 are calculated from the available failure stresses, assuming a linear behavior up to failure in material directions.

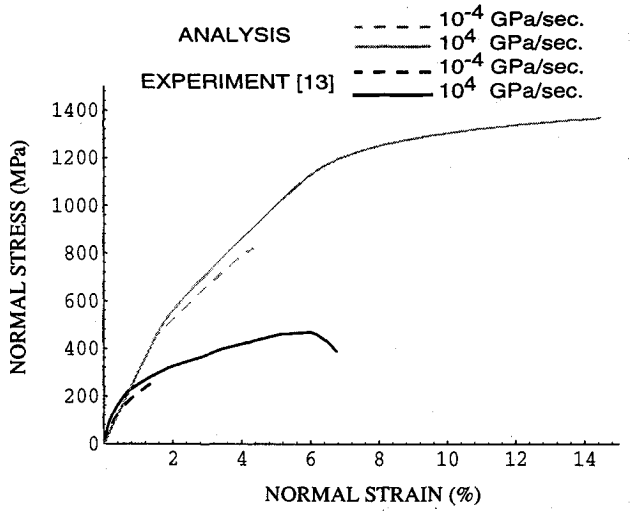

Fig. 9 Comparison of the analytical and experimental stress-strain relation for ± 30 angle-ply laminate (analysis—SP250/S-2 glass/epoxy, experiment—Scotchply 1002 glass/epoxy).

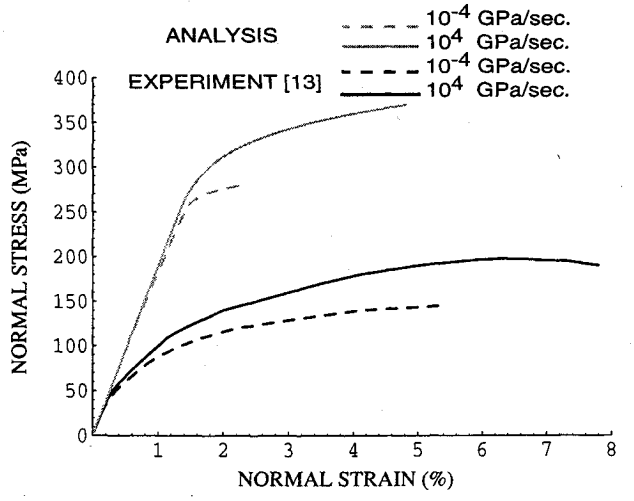

Fig. 10 Comparison of the analytical and experimental stress-strain relation for ± 45 angle-ply laminate (analysis—SP250/S-2 glass/epoxy, experiment—Scotchply 1002 glass/epoxy).

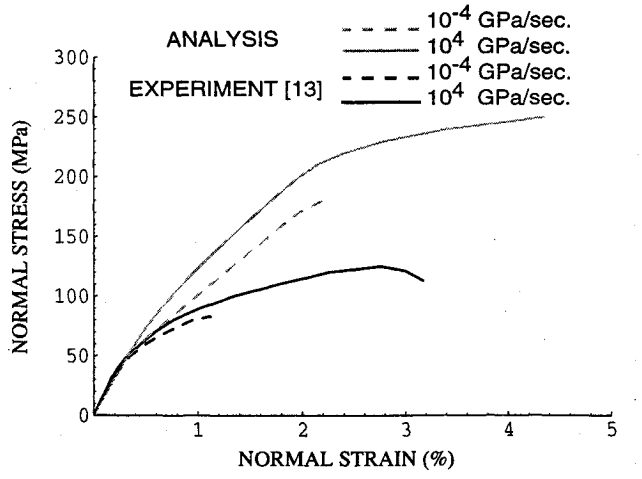

Fig. 11 Comparison of the analytical and experimental stress-strain relation for ± 60 angle-ply laminate (analysis—SP250/S-2 glass/epoxy, experiment—Scotchply 1002 glass/epoxy).

Conclusions

Damage evolution in a laminated composite under quasistatic random loading is discussed in this paper. The analysis shows that laminate failure strength increases with the increase of the loading rate, in general. Failure strain also increases, and deformation behavior shows increasing nonlinearity with loading rate. The shift in damage accumulation onset and the stretching of the stress interval of damage accumulation with the increase in loading rates are also observed. An increase in loading rate can cause qualitative changes in the damage sequence. The cumulative damage content at failure varies slightly with the loading rate. Analysis shows that the behavior of failure stress and strain with respect to the loading rate is strongly affected by loading deviation. It is seen that shear-extension coupling coefficients may become fairly big due to damage accumulation and affect the stress-strain behavior and failure stress of the laminate. The analytical results are qualitatively similar to the available experimental observations.

Acknowledgments

This work is funded by the Army Research Office. The project monitor is G. L. Anderson. Y. A. Dzenis would like to thank his wife, Natasha Dzenis, for patience.

References

[1]Ovchinskii, A. S., *Fracture Processes in Composite Materials: Computer Imitation of Micro- and Macromechanisms*, Nauka Publishers, Moscow, 1988 (in Russian).

[2]Wagner, H. D., "Statistical Concepts in the Study of Fracture Properties of Fibres and Composites," *Application of Fracture Mechanics to Composite Materials*, edited by K. Friedrich, Vol. 6, Composite Materials Series, Elsevier, New York, 1989, pp. 39–77.

[3]Argon, A., "Statistical Aspects of Fracture," *Fracture and Fatigue*, Vol. 5, Composite Materials Series, Academic Press, New York, 1974, pp. 166–205.

[4]Bogdanovich, A. E., and Yushanov, S. P., "Buckling Analysis of Cylindrical Shells Having Random Field of Initial Imperfections Under Axial Dynamic Compression," *Mechanics of Composite Materials* (Riga), No. 5, 1981, pp. 821–831.

[5]Bogdanovich, A. E., and Yushanov, S. P., "On the Calculation of Reliability Function of Anisotropic Shells by Using Technique of Seldom Outbursts of a Stochastic Vector Field out of the Limiting Surface," *Mechanics of Composite Materials* (Riga), No. 1, 1983, pp. 80–89.

[6]Yushanov, S. P., and Bogdanovich, A. E., "Method of Reliability Calculation for Imperfect Laminated Cylindrical Shells with Account for Scatter of Composite Strength Characteristics," *Mechanics of Composite Materials* (Riga), No. 6, 1986, pp. 1043–1048.

[7]Yushanov, S. P., "On Reliability Calculation of Laminated Composite Shells with Random Elastic and Strength Characteristics," *Mechanics of Composite Materials* (Riga), No. 1, 1985, pp. 87–96.

[8]Yushanov, S. P., "Probabilistic Model of Composite Ply-by-Ply Failure and Reliability Calculation of Laminated Cylindrical Shells," *Mechanics of Composite Materials* (Riga), No. 1, 1985, pp. 642–652.

[9]Bogdanovich, A. E., and Yushanov, S. P., "A Reliability Analysis of Laminated Composites and Cylindrical Shells," *Proceedings of the Sixth International Conference on Composite Materials and Second European Conference on Composite Materials*, Vol. 5, Elsevier, London, 1987, pp. 5.525–5.535.

[10]Dzenis, Y. A., Joshi, S. P., and Bogdanovich, A. E., "Damage Evolution Modeling in Orthotropic Laminated Composites," *Proceedings of the AIAA/ASME/ASCE/AHS/ASC 33rd Structures, Structural Dynamics, and Materials Conference*, Pt. 5, AIAA, Washington, DC, 1992, pp. 2887–2897.

[11]Sveshnikov, A. A., *Applied Methods of the Theory of Random Functions*, Nauka Publishers, Moscow, 1968 (in Russian).

[12]Clements, L. L., and Chiao, T. T., "Engineering Design Data for an Organic Fiber/Epoxy Composite," *Composites*, Vol. 8, No. 2, 1977, pp. 87–92.

[13]Staab, G. H., and Gilat, A., "Behavior of Angle-Ply Glass/Epoxy Laminates under Tensile Loading at Quasi-Static and High Rates," *Proceedings of the Seventh Technical Conference of the American Society for Composites*, Technomic Publishing, Westport, CT, 1992, pp. 1041–1050.